

## Non-equilibrium signals of the $SU(3)$ deconfining phase transition

---

**Alexei Bazavov\* and Bernd A. Berg**

*Department of Physics, Florida State University, Tallahassee, FL 32306-4350, USA*

*School of Computational Science, Florida State University, Tallahassee, FL 32306-4120, USA*

**Alexander Velytsky**

*Department of Physics and Astronomy, UCLA, Los Angeles, CA 90095-1547, USA*

In  $SU(3)$  simulations with the model A (Glauber) dynamics we find unambiguous signal for the transition when the (driving) temperature  $T_f$  is larger than  $T_c$ . A dynamical growth of Polyakov loop structure factors, reaching maxima which scale approximately with the volume of the system, precedes equilibration. We study their influence on various observables, using different lattice sizes to illustrate an approach to a finite volume continuum limit. Strong correlations are found during the dynamical process, but not in the deconfined phase at equilibrium. Debye screening masses  $m_D(T_f)$  are estimated from initial response to the temperature change and found to be consistent with equilibrium estimates by Kaczmarek et al.

*XXIVth International Symposium on Lattice Field Theory*

*July 23-28, 2006*

*Tucson, Arizona, USA*

---

\*Speaker.

## 1. Introduction

In investigations of the QCD deconfining phase transition (or crossover) by means of heavy-ion experiments, one ought also to be concerned about non-equilibrium effects due to the *rapid heating* of the system [1]. The QCD high temperature vacuum is characterized by ordered Polyakov loops, which are similar to spins in the low temperature phase of the 3D 3-state Potts model. We model heating by a quench from the disordered into the ordered phase. Time evolution after the quench leads to vacuum domains of distinct triality under the  $Z_3$  center of the  $SU(3)$  gauge group. It appears that these competing domains are the underlying cause for the explosive growth of structure factors  $F_i(t)$ , which we encounter in the time evolution after a heating quench. We use the term *spinodal decomposition* loosely to denote generically such a time period of globally unstable behavior.

Relaxation of the system at its new temperature becomes only feasible after each structure factor has overcome its maximum value. While the maximum value of the structure factor diverges with lattice size, its initial and final equilibrium values are finite in the normalization chosen in the paper. The time (measured in updates per degree of freedom) for reaching the maximum diverges with lattice size unless the underlying order-order symmetry is broken. Once the system has equilibrated at high temperature, the subsequent temperature falloff is driven by spatial lattice expansion and the system stays in quasi-equilibrium during this period. So one has different time scales under heating and cooling [2].

The early time evolution of  $SU(3)$  gauge theory after the quench is well described by stochastic equations, which follow from dynamical generalizations of equilibrium Landau-Ginzburg effective action models. We calculate the exponential growth factor of this linear approximation and use a phenomenological model [3] to estimate the Debye screening mass for two temperatures above the deconfining  $T_c$ .

Finally we compare measurements of Polyakov loop correlations, gluonic energy densities and pressures around structure function maxima with their equilibrated values in the deconfined region at high temperatures. These measurements are of interest for a scenario in which the heating process turns back to cooling before actually reaching the equilibrium side of the structure factor maxima. In the conclusions we continue this discussion.

## 2. Notation and Preliminaries

We simulate pure  $SU(3)$  non-Abelian Euclidean lattice gauge theory with the Wilson action

$$S_A = \frac{2 \cdot 3}{g^2} \sum_{n,\mu\nu} \left[ 1 - \frac{1}{2 \cdot 3} \text{Tr}(U_{n,\mu\nu} + \text{h.c.}) \right], \quad (2.1)$$

where  $U_{n,\mu\nu} = U_{n,\mu} U_{n+\hat{\mu},\nu} U_{n+\hat{\nu},\mu}^\dagger U_{n,\nu}^\dagger$  denotes the product of the  $SU(3)$  link matrices in the fundamental representation around a plaquette and the sum runs over all plaquettes. Simulations are carried out on  $N_\tau N_\sigma^3$  lattices. Lattice size in physical units is denoted  $L = a N_\sigma$ , where  $a$  is the lattice spacing.

The Markov chain Monte Carlo (MC) process provides model A (Glauber) dynamics in the classification of Ref. [4]. We use the Cabibbo-Marinari [5] heatbath algorithm and its improvements of Ref. [6] (no over-relaxation, to stay in the universality class of Glauber dynamics). A

time step is a sweep of systematic updating through the lattice, which touches each degree of freedom once.

Polyakov loop is defined as a trace of a product of  $SU(3)$  matrices in  $N_\tau$  direction, and its lattice average is the order parameter of pure gauge theory:

$$P(\vec{x}) = \text{Tr} \prod_{i=0}^{N_\tau-1} U_{\vec{x},i}, \quad \langle P \rangle_L = \frac{1}{N_\sigma^3} \sum_{\vec{x}} P(\vec{x}). \quad (2.2)$$

Lattice averaged correlation function of Polyakov loops is denoted:

$$\langle P(0)P^\dagger(\vec{x}) \rangle_L = \frac{1}{N_\sigma^3} \sum_{\vec{i}} P(\vec{i})P^\dagger(\vec{i}+\vec{x}). \quad (2.3)$$

The Fourier transform of (2.3) is called structure function and in discretized version is

$$F(\vec{p}) = \frac{a^3}{N_\sigma^3} \left| \sum_{\vec{x}} e^{-i\vec{k}\vec{x}} P(\vec{x}) \right|^2. \quad (2.4)$$

As we let the system evolve after a quench  $P(\vec{x})$  becomes time-dependent:  $P(\vec{x}, t)$ . The time  $t$  corresponds to the dynamical process, i.e., in our case the Markov chain model A dynamics. We consider an ensemble of systems (replica) and dynamical observables are calculated as ensemble averages denoted by  $\langle \dots \rangle$ . The time-dependent structure functions averaged over replicas are  $F_{\vec{p}}(t) = \langle F(\vec{p}, t) \rangle$ . We use the notation  $F_i(t)$  to represent a structure function at momentum  $\vec{p} = \vec{k}/a = 2\pi\vec{n}/L$ , where  $|\vec{n}| = n_i$  defines  $i$ . The  $F_i$  are called structure function modes or structure factors (SFs).

### 3. Evolution in $SU(3)$ Pure Gauge Theory

We report the results from quenches on different lattices with  $N_\tau = 4, 6, 8$ . All quenches are from the initial value  $6/g^2 = 5.5$ . The data serve to study the quantum continuum limit  $a \rightarrow 0$  (in physical units like fermi). The final values  $g_f^2$  of the bare coupling constants are chosen, so that the values of  $T_f/T_c$  stay at the fixed ratios: 1.25 and 1.568 for the present study. For this we take (substantial) corrections to the two-loop equation of Lambda lattice into account. Details, lattice sizes and gauge coupling values used are given in [1].

#### 3.1 Finite Volume Continuum Limit

Infinite volume limit  $N_\tau = \text{const}$ ,  $N_\sigma \rightarrow \infty$  was extensively studied for Potts models and for  $SU(3)$  pure gauge theory [1]. In the following we illustrate the approach of the limit  $a \rightarrow 0$ ,  $L = \text{constant}$ ,  $T_f/T_c = \text{constant}$ , by increasing  $N_\tau$  from 4 to 6 to 8 and the volume  $N_\sigma^3$  from  $N_\sigma = 16$  to 24 to 32, so that the ratio  $N_\sigma/N_\tau$  stays constant. Due to the divergence of (bare) Polyakov loop correlations we face a renormalization problem, which we overcome by dividing all SFs  $F_i$  by their equilibrium values at  $T_f$ ,  $F_{i,f}$ . The time-scale situation changes too, because we have to use different bare coupling constant values for different  $N_\tau$ . As one knows, a finite physical volume equilibrates in a finite time, we fix this normalization problem by rescaling the time axis to

$$t' = \frac{t}{\lambda_t(N_\tau, T_f/T_c)} \quad (3.1)$$

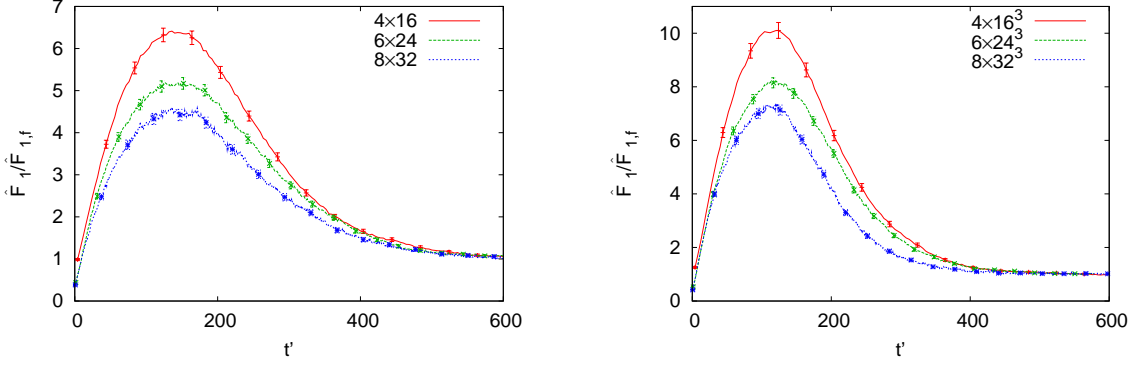


**Figure 1:** Time evolution of SF  $F_1/F_{1,f}$  for SU(3) lattice gauge theory on  $N_\tau N_\sigma^3$  lattices of constant physical volume of a quench to  $T_f/T_c = 1.25$  (left) and  $T_f/T_c = 1.568$  (right).

so that all maxima fall on top of one another.

Figure 1 shows the time evolution of the  $F_1/F_{1,f}$  SFs for our two  $T_f/T_c$  values. Rescaling factors are  $\lambda_t(N_\tau, 1.25) = 1 : 2.655 : 5.457$  and  $\lambda_t(N_\tau, 1.568) = 1 : 2.768 : 6.362$  for the  $N_\tau$  values 4 : 6 : 8, respectively. The maxima of the curves decrease when increasing  $N_\tau$  from 4 to 6 to 8. As the decrease slows down with increasing lattice size, there is some evidence for an approach to a shape, which represents the continuum limit.

### 3.2 Debye Screening Mass

The current understanding of the early time evolution of systems out of equilibrium is largely based on investigating stochastic equations which are dynamical (time dependent) generalizations of the Landau-Ginzburg effective action models of the static (equilibrium) theory. For model A the linear approximation results in the following early growth of SFs:

$$\begin{aligned} \hat{F}(\vec{p}, t) &= \hat{F}(\vec{p}, t=0) \exp(2\omega(\vec{p})t), \\ \omega(\vec{p}) &> 0 \text{ for } |\vec{p}| > p_c, \end{aligned} \quad (3.2)$$

where  $p_c > 0$  is a critical momentum (for details of linear theory for model A see Ref. [7]).

From our measurements of  $F(\vec{p}, t)$  on the  $N_\tau = 4, 6$  and 8 lattices we find straight line fits to the form  $\omega(p) = a_0 + a_1 p^2$ ,  $p = |\vec{p}|$  with a negative slope  $a_1$ . They determine the critical momentum  $p_c$  as the value where  $\omega(p)$  changes its sign. The fits for  $T_f/T_c = 1.25$  and for  $T_f/T_c = 1.568$  are shown in Fig. 2, where we introduced  $\omega'(p) = \lambda_t(N_\tau, T_f/T_c) \omega(p)$ . This definition absorbs the shift (3.1) of the time scale, so that  $\omega'(p)t' = \omega(p)t$  holds. The obtained values for  $p_c(N_\tau)/T_c$  are listed in table 1. The (finite volume) continuum limit is extrapolated by fitting these values to the form

$$\frac{p_c(N_\tau)}{T_c} = \frac{p_c}{T_c} + \frac{\text{const}}{N_\tau} \quad (3.3)$$

with the results given in the fifth column of table 1.

Relying on a phenomenological analysis by Miller and Ogilvie [3],  $p_c$  is related by  $m_D = \sqrt{3} p_c$  to the Debye screening mass at the final temperature  $T_f$  after the quench, shown in the last

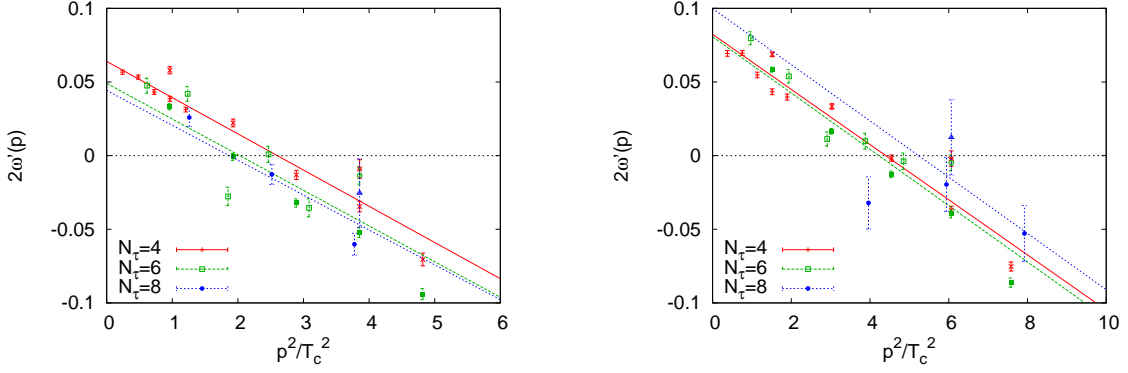


**Figure 2:**  $SU(3)$  determination of  $p_c$  for  $T_f/T_c = 1.25$  (left) and  $T_f/T_c = 1.568$  (right).

**Table 1:** Fit results for  $p_c/T_c$ .

Lattice size:	$N_\tau = 4$	$N_\tau = 6$	$N_\tau = 8$	$\infty$	$m_D$
$T_f/T_c = 1.25$ :	1.613 (18)	1.424 (26)	1.37 (10)	1.058 (79)	$1.83(14) T_c$
$T_f/T_c = 1.568$ :	2.098 (19)	2.058 (22)	2.29 (15)	2.006 (73)	$3.47(13) T_c$

column of table 1. The value at  $T_f/T_c = 1.568$  is in excellent agreement with a determination of  $m_D(T)$  from a best-fit analysis of the large distance part of the color singlet free energies on equilibrium configurations by Kaczmarek et al. [8]. This supports the idea that the simulated dynamics bears physical content. Our estimate at  $T_f/T_c = 1.25$  is by a factor of two smaller than the one of Ref. [8]. But this is not really a surprise, because  $T_f/T_c = 1.25$  is close to the spinodal endpoint, so that the derivation [3] of the relationship between  $m_D$  and  $p_c$  is no longer valid. The screening length associated with the Debye mass,  $\xi_D = 1/m_D$ , is then approximately 0.6 fermi at  $T_f/T_c = 1.25$  and 0.3 fermi at  $T_f/T_c = 1.568$ . Our result is that the Debye screening length is short on the scale of the deconfined region envisioned to be about  $10^3 \text{ fm}^3$  in relativistic heavy-ion experiments.

### 3.3 Measurements near Structure Factor Maxima versus Deconfined Equilibrium

For  $SU(3)$  gauge theory the triality of Polyakov loops with respect to the  $Z_3$  center of the gauge group takes the place of the spin orientations in the 3D 3-state Potts model. Although a satisfactory cluster definition does not exist for gauge theories (see [9] for some progress), the underlying mechanism of competing vacuum domains is expected to be similar to the one in spin models. Indirect indication of such a mechanism is presented in Fig. 3 where we plot histograms of the order parameter at different time steps during the evolution:  $t = 0$ ,  $t = t_{max}$  and  $t = 5t_{max}$  ( $t_{max}$  represents a time step when SFs reach maxima). The histograms are normalized to have the same height on all three plots. At  $t = 0$  all systems (replica) in the ensemble are in the confined phase so the Polyakov loop fluctuates around zero. At  $t = t_{max}$  the order parameter shifts to non-zero values. Some replica "move" toward each of the three final values, but some other have the Polyakov loop value somewhat "in between": due to the competition of different domains those systems have not decided yet which final value of the order parameter is to be assumed. At  $t = 5t_{max}$  the ensemble is clearly in equilibrium with one third (on average) of the replica assuming each possible

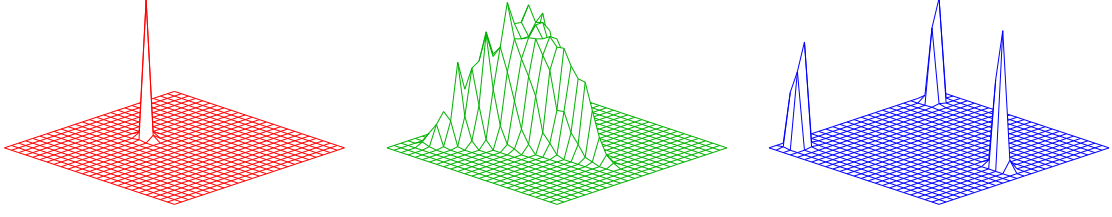


**Figure 3:** The histograms of the order parameter value at  $t = 0, t_{max}, 5t_{max}$  (left to right) on  $6 \times 24^3$  lattice.

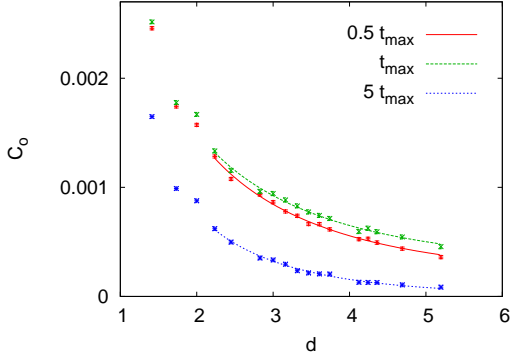


**Figure 4:** Fall-off behavior of the Polyakov loop correlations at  $T_f/T_c = 1.25$  at different times.

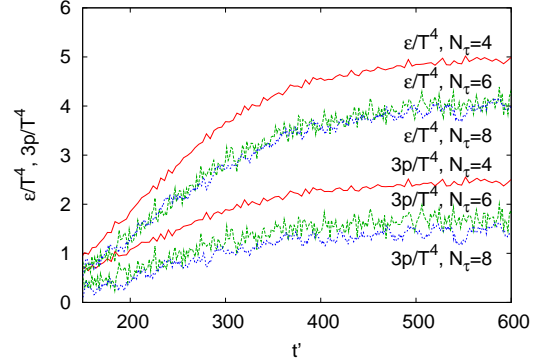


**Figure 5:**  $SU(3)$  gluonic energy densities and pressures at  $T_f/T_c = 1.25$ .

Polyakov loop value. To study how the the existence of different domains influences Polyakov loop correlations and the gluonic energy  $\varepsilon$  and pressure  $p$  densities, we calculate these quantities at times  $t \leq t_{max}$  as well as at  $t > t_{max}$ .

During the quench we measure two-point correlations between Polyakov loops defined by

$$C_o(d, t) = \langle P(0, t)P(d, t) \rangle_L - (\langle |P(0, t)| \rangle_L)^2. \quad (3.4)$$

Their fall off with distance at different times is shown in Fig. 4. At  $5t_{max}$  (in equilibrium) it is exponential (as expected). In contrast to that large correlations are found at  $0.5t_{max}$  and  $t_{max}$ , which are fully consistent with a power law.

The equilibrium procedure for calculating the gluonic energy  $\varepsilon$  and pressure  $p$  densities is summarized in Ref. [10, 11]. We calculate their evolution during the quench along the same lines. In Fig. 5 we show the time evolution of the gluonic energy densities (upper curves) and pressure densities (lower curves) for the  $T_f/T_c = 1.25$  quench on our  $4 \times 16^3$ ,  $6 \times 24^3$  and  $8 \times 32^3$  lattices using the rescaled time definition (3.1). The curves for the last two lattices fall almost on top of one another, indicating their neighborhood to the continuum limit. The approach to the final equilibrium values is rather smooth and takes about the same time as equilibration of the structure factors.

#### 4. Summary and Conclusions

In equilibrium at temperatures much higher than the deconfinement temperature  $T_c$  the perturbative prescription of QCD is that of a weakly coupled gas of quasiparticles. In contrast, recent experiments at the BNL relativistic heavy-ion collider (RHIC) show coherence in particle production and strong collective phenomena, which are well described by the model of a near-perfect, strongly coupled fluid [12]. Nonperturbative effects are expected to play some role in the prescription of equilibrium QCD at temperatures reached at RHIC. For the  $T_f/T_c = 1.25$  and  $T_f/T_c = 1.568$  temperatures investigated in this paper equilibrium lattice calculations indeed indicate corrections (compare Fig. 7 of [10]). However correlations are typically over ranges much smaller than the size of the deconfined plasma, compare our estimates of the Debye screening mass  $m_D(T_f)$ . So one should not *a-priori* exclude the possibility that, under heating, the system did not reach true equilibrium, but instead got stuck in the neighborhood of the SF maxima of the spinodal decomposition.

#### Acknowledgments

This work was in part supported by the DOE grant No. DE-FG02-97ER41022 at FSU and the No. NSF-PHY-0309362 grant at UCLA. The simulations were performed on PC clusters at FSU and UCLA.

#### References

- [1] A. Bazavov, B.A. Berg, and A. Velytsky, Phys. Rev. D **74**, 014501 (2006) and references therein.
- [2] E.T. Tomboulis and A. Velytsky, Phys. Rev. D **72**, 074509 (2005).
- [3] T.R. Miller and M.C. Ogilvie, Nucl. Phys. B (Proc. Suppl.) **106** (2002) 537; Phys. Lett. B **488** (2000) 313.
- [4] P.M. Chaikin and T.C. Lubensky, *Principles of condensed matter physics* (Cambridge University Press, Cambridge, 1997), table 8.6.1, p.467.
- [5] N. Cabibbo and E. Marinari, Phys. Lett. **B119**, 387 (1982).
- [6] K. Fabricius and O. Hahn, Phys. Lett. **B143**, 459 (1984); A.D. Kennedy and B.J. Pendleton, Phys. Lett. **B156**, 393 (1985).
- [7] B.A. Berg, H. Meyer-Ortmanns, and A. Velytsky, Phys. Rev. D **70**, 054505 (2004).
- [8] O. Kaczmarek, F. Karsch, F. Zantow, and P. Petreczky, Phys. Rev. D **70**, 074505 (2004); O. Kaczmarek and F. Zantow, Phys. Rev. D **71**, 114510 (2005).
- [9] S. Fortunato, J. Phys. A **36**, 4269 (2003).
- [10] G. Boyd, J. Engels, F. Karsch, E. Laermann, C. Legeland, M. Lütgemeier, and B. Peterson, Nucl. Phys. **B469**, 419 (1996).
- [11] J. Engels, F. Karsch, and T. Scheideler, Nucl. Phys. **B564**, 303 (2000).
- [12] U.W. Heinz, AIP Conf. Proc. **739**, 163 (2004); P.F. Kolb, Acta Phys. Hung. N.S. **21**, 243 (2004); P.F. Kolb and U.W. Heinz, *Hydrodynamic Description of Ultrarelativistic Heavy-Ion Collisions in Quark Gluon Plasma 3*, R.C. Hwa and X.N. Wang, Editors (World Scientific, Singapore, 2004); nucl-th/0305084.